

# 2023 IC Fabrication MOSFETs, Inverters, and Ring Oscillators - Group 1

Richard A. McManus, Jr.

**Abstract**—This document presents the characterization of metal oxide semiconductor field effect transistors (MOSFETs), complimentary metal oxide semiconductor (CMOS) inverters, and ring oscillators fabricated by Group 1 in the University of Notre Dame's course, IC Fabrication, taught by Dr. Alan Seabaugh. 1.5 $\mu$ m, 2 $\mu$ m, and 3 $\mu$ m, gate length n-channel and p-channel MOSFETs were fabricated and tested in the Notre Dame Nanofabrication Facility. Subthreshold swings of 714 mV/dec and 104 mV/dec and threshold voltages of 1.56 V and 2.64 V were measured for 1.5 $\mu$ m n-channel and p-channel MOSFETs respectively. A static noise margin (SNM) of 1.7 V was measured from a 1.5 $\mu$ m inverter. Fundamental, third, and fifth harmonics were observed multiple 61-stage ring oscillators of various gate lengths.

**Index Terms**—MOSFET, Inverter, Ring Oscillator, Transmission Line Measurement, Static Noise Margin

## I. INTRODUCTION

FOLLOWING the recent enactment of the United States CHIPS and Science Act of 2022, opportunity is growing for American engineers with experience in semiconductor processing. IC Fabrication, a course created by Dr. Gregory Snider and currently taught by Dr. Alan Seabaugh at the University of Notre Dame, provides aspiring students with hands-on experience in the semiconductor process. Across three months, students work in groups of three and spend nearly 100 hours in the Notre Dame Nanofabrication Facility to take bare silicon wafers through an 18 step process yielding MOSFETs, Inverters, and Ring Oscillators. This document presents the characterization of those fabricated devices.

## II. OPTICAL MICROSCOPE ANALYSIS

Fig. 1 shows an optimal micrograph of three n-channel MOSFETs fabricated by group 1 with gate lengths of 3 $\mu$ m, 2 $\mu$ m, 1.5 $\mu$ m. The MOSFETs have a width of 20 $\mu$ m. Proper alignment is demonstrated between the gate oxide and aluminum metal layer. A single gate via is visible below the MOSFETs. A body via connected to the p-type well is visible to the right of the MOSFETs. A similiar structure for the characterization of p-channel MOSFETs was fabricated.

Fig. 2 shows four CMOS inverters with gate lengths of 3 $\mu$ m, 2 $\mu$ m, 1.5 $\mu$ m, and 1 $\mu$ m. Proper alignment was demonstrated for all four inverters and promising results were obtained for each.

Manuscript received 7 December 2023; date of current version 7 December 2023. (Corresponding author: Richard A. McManus, Jr.)

These devices work fabricated as part of the course, IC Fabrication, in the Notre Dame Nanofabrication Facility.

R.A. McManus, Jr. is with the University of Notre Dame, Notre Dame, IN 46556 USA (e-mail: rmcmanu2@nd.edu).

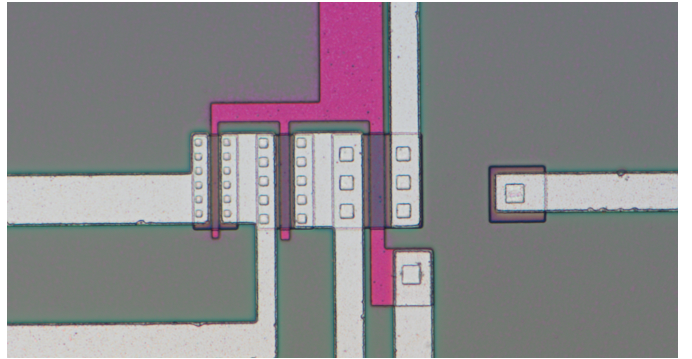


Fig. 1. Optical Micrograph of fabricated n-channel MOSFETs with gate lengths of 3 $\mu$ m, 2 $\mu$ m and 1.5 $\mu$ m.

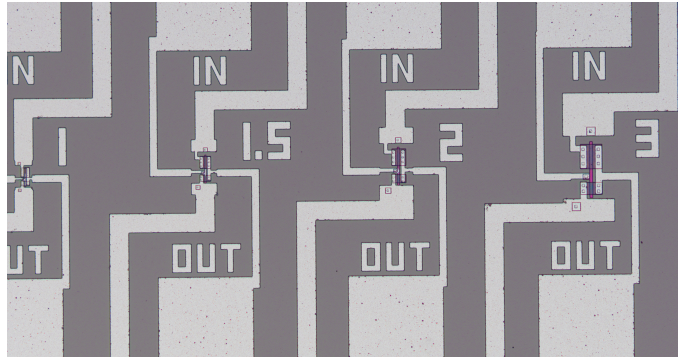


Fig. 2. Optical Micrograph of fabricated inverters with gate lengths of 3 $\mu$ m, 2 $\mu$ m, 1.5 $\mu$ m, and 1 $\mu$ m.

## III. MOSFET CHARACTERISTICS

The common source current-voltage relationships and transfer functions for the n-channel and p-channel MOSFETs were obtained using the Keysight B1500A Semiconductor Device Parameter Analyzer. The characteristics for the 1.5 $\mu$ m gate length devices are presented below.

Fig. 3, shows the measured common source current-voltage relationships for various gate to source voltages ( $V_{GS}$ ) of the 1.5 $\mu$ m n-channel MOSFET. Leakage is observed at high values of  $V_{GS}$ , yielding additional current in the saturation region. The transfer function of the 1.5 $\mu$ m n-channel MOSFET, shown in Fig. 4, was measured to determine a subthreshold swing (SS) of 714 mV/dec and threshold voltage ( $V_{TH}$ ) of 1.56 V for  $V_{DS} = 3.1V$  and  $V_{GS} = 0.7V$  [1].

Fig. 5 provides the common source current-voltage relationships for various  $V_{GS}$  of the 1.5 $\mu$ m p-channel MOSFET. From the lower hole-mobility, less current is observed in the

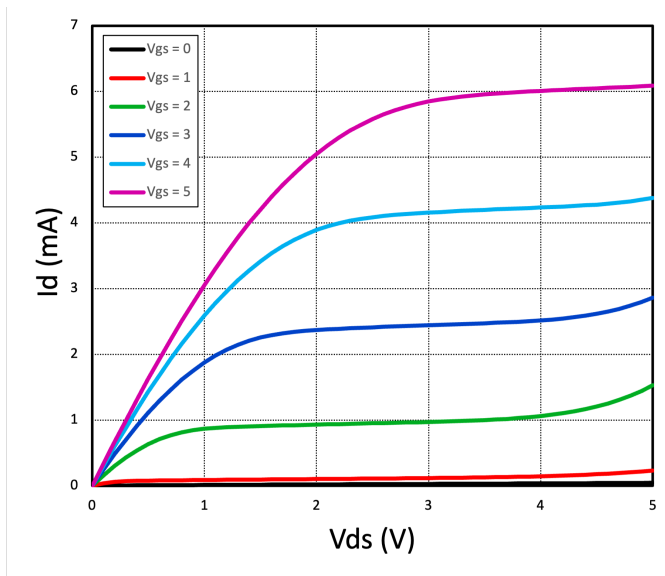


Fig. 3. Common source current-voltage ( $Id$  -  $Vgs$ ) relationship of  $1.5\mu\text{m}$  n-channel MOSFET.

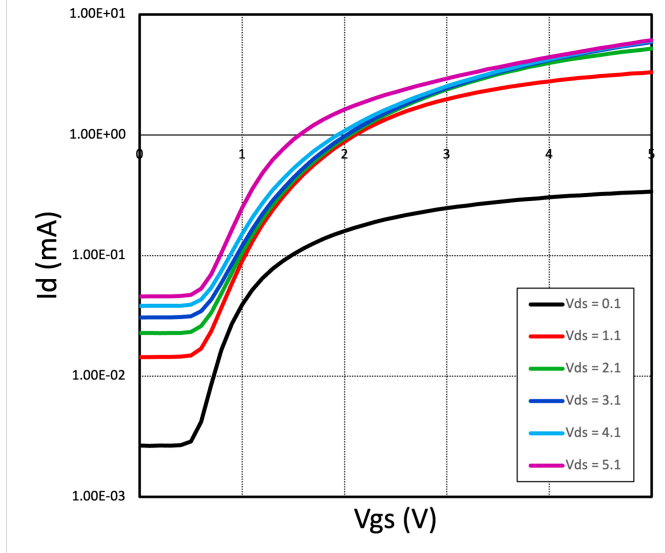


Fig. 4. Transfer characteristics of  $1.5\mu\text{m}$  n-channel MOSFET

p-channel device. There is also less leakage current present at high values of  $Vgs$ . The transfer function of the  $1.5\mu\text{m}$  p-channel MOSFET, shown in Fig. 6, was measured to determine a subthreshold swing (SS) of  $104 \text{ mV/dec}$  and threshold voltage ( $Vth$ ) of  $2.64 \text{ V}$  for  $Vds = -3.1\text{V}$  and  $Vgs = -1.4\text{V}$ .

Using an oxide thickness of  $15 \text{ nm}$ , measured during fabrication, and the previously provided threshold voltages, the expected drain currents, shown in Fig. 7, were calculated for both devices. The calculated saturation currents for high values of  $Vgs$  were significantly higher than the measured values. This is most likely caused by lower mobilities than expected from impurities in the device.

#### IV. TRANSMISSION LINE MEASUREMENTS

Transmission line measurements (TLM) were taken from polysilicon, n-well, and p-well regions and are shown in Fig. 8.

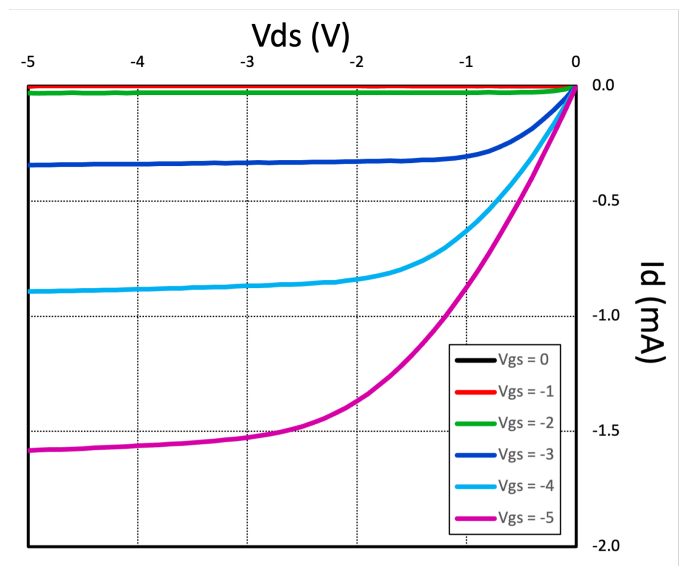


Fig. 5. Common source current-voltage ( $Id$  -  $Vgs$ ) relationship of  $1.5\mu\text{m}$  p-channel MOSFET.

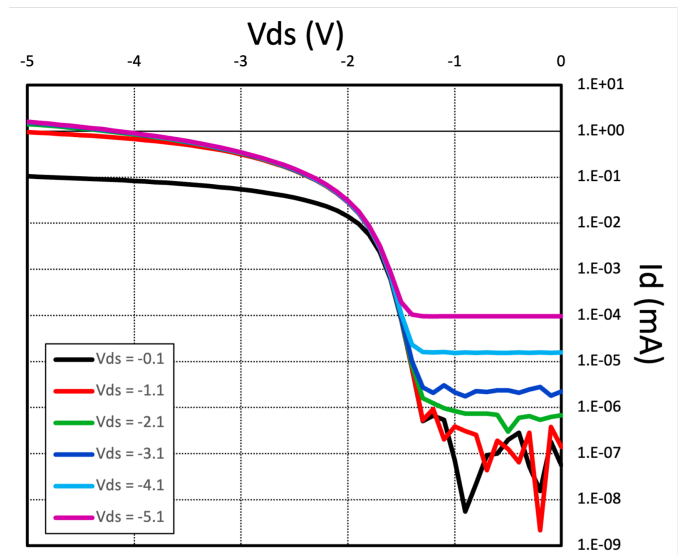


Fig. 6. Transfer characteristics of  $1.5\mu\text{m}$  p-channel MOSFET

Contact resistances of  $13$ ,  $9$ , and  $8 \text{ ohms}$  and sheet resistances of  $39$ ,  $48$ , and  $58 \text{ ohms}$  were measured for the polysilicon, n-well, and p-well respectively. Measurement values for the n-well and p-wells were rather linear. The polysilicon resistance measurements; however, were nonlinear. Further characterization may be required to determine more accurate results.

#### V. INVERTER CHARACTERISTICS

All four fabricated inverters,  $3\mu\text{m}$ ,  $2\mu\text{m}$ ,  $1.5\mu\text{m}$ , and  $1\mu\text{m}$  gate length, performed well. A butterfly curve generated from the voltage transfer characteristics of a  $1.5\mu\text{m}$  inverter is shown in Fig. 9. An SNM of  $1.7 \text{ V}$  was determined from the largest square capable of fitting within both lobes.

$ V_{gs} $ (V)	NMOS Calculated $ Id $ (mA)	NMOS Measured $ Id $ (mA)	PMOS Calculated $ Id $ (mA)	PMOS Measured $ Id $ (mA)
0	0	0	0	0
1	0	0.2	0	0
2	0.3	1	0	0.1
3	3	2.4	1	0.3
4	9	4.3	4	0.8
5	18	6	8	1.6

Fig. 7. Comparison of Calculated and Measured 1.5μm MOSFET Drain Currents

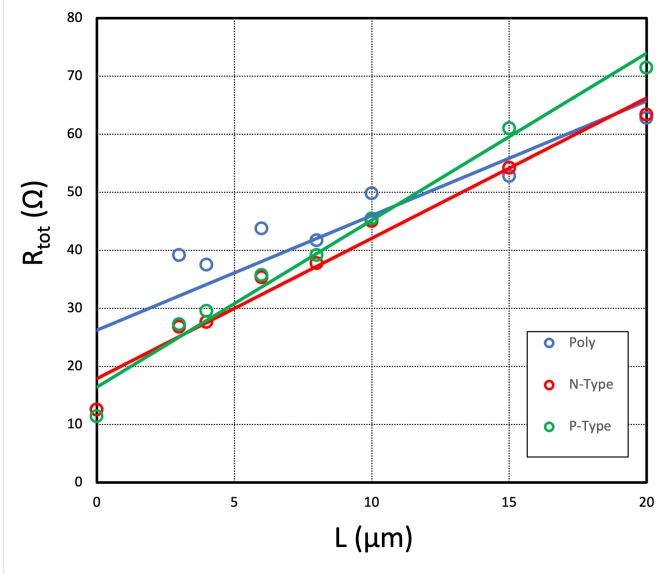


Fig. 8. Transmission line measurements of polysilicon, p-well, and n-well

## VI. OSCILLATOR PERFORMANCE

2μm, 1.5μm, 1μm, and 0.75μm ring oscillators successfully demonstrated instability. A 14.7 MHz oscillation is shown in Fig. 10, generated by a 2μm oscillator with an input voltage of 10.7 V. This corresponds to a propagation delay of 557 ps. Third and fifth harmonics, shown in Fig. 11 and Fig. 12 respectively, were observed in the devices. The presence of these harmonics suggest more than one transition state is occurring within these oscillators [2], [3]. The various amplitudes of these harmonics can be explained by non-equidistant transition states. The number of stages between transition states can be determined by

$$N = \frac{t_{n1-n2}}{t_{pd}}$$

where  $t_{n1-n2}$  is the time between a set of adjacent peaks and valleys of the output waveform and  $t_{pd}$  is the inverter propagation delay found from the fundamental frequency.

## VII. CONCLUSION

Group 1 successfully demonstrated functionality in all fabricated devices. 1.5μm gate length N-channel and p-channel MOSFETs yielded drain currents as high as 6 mA and 1.5

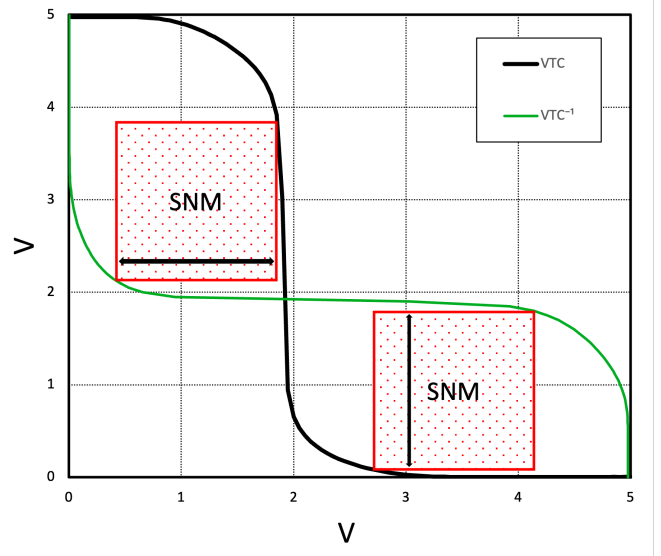


Fig. 9. Butterfly curve 1.5μm inverter voltage transfer characteristics

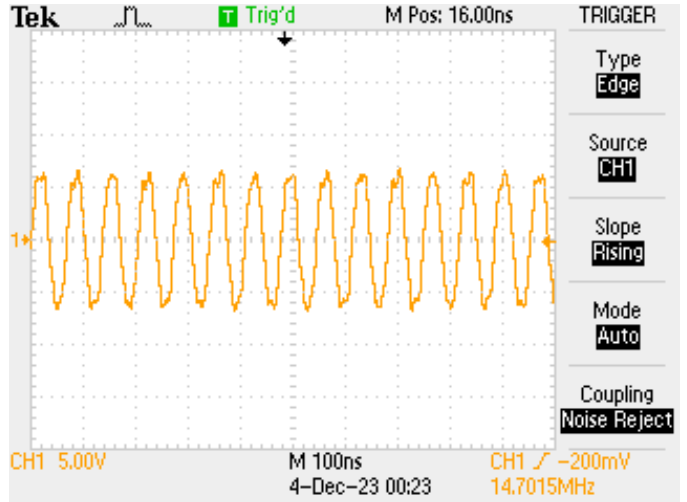


Fig. 10. 14.7 MHz oscillation generated by a 2μm oscillator with an input voltage of 10.7 V

mA respectively. A static noise margin of 1.7 V was measured from a 1.5μm gate length inverter, and ring oscillators with gate lengths of 2μm, 1.5μm, 1μm, and 0.75μm all produced output waveforms. As this process represented Group 1's introduction to semiconductor fabrication, the characteristics of the presented devices are promising. Many of the group members will continue to refine their fabrication skills through undergraduate research this spring.

## REFERENCES

- [1] Cheng, Z., Pang, CS., Wang, P. et al. How to report and benchmark emerging field-effect transistors. Nat Electron 5, 416–423 (2022). <https://doi.org/10.1038/s41928-022-00798-8>
- [2] N. Sasaki, "Higher harmonic generation in CMOS/SOS ring oscillators," in IEEE Transactions on Electron Devices, vol. 29, no. 2, pp. 280-283, Feb. 1982, doi: 10.1109/T-ED.1982.20696.
- [3] J. P. Caram, J. Galloway and J. S. Kenney, "Time-to-Digital Converter With Sample-and-Hold and Quantization Noise Scrambling Using Harmonics in Ring Oscillators," in IEEE Transactions on

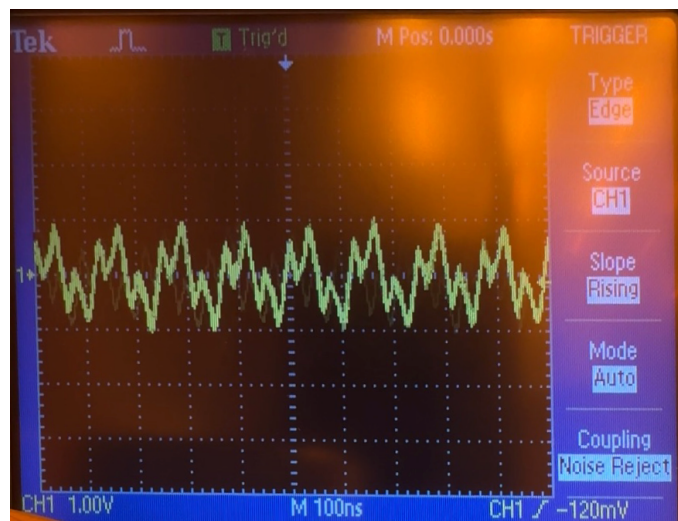


Fig. 11. Presence of third harmonic in  $0.75\mu\text{m}$  Ring Oscillator



Fig. 12. Presence of fifth harmonic in  $2\mu\text{m}$  Ring Oscillator

Circuits and Systems I: Regular Papers, vol. 65, no. 1, pp. 74-83, Jan. 2018, doi: 10.1109/TCSI.2017.2712518.